A R C H I V E S O F M E T A L L U R G Y A N D M A T E R I A L S
Volume 60 2015 Issue 4
DOI: 10.1515/amm-2015-0465

A. LISIECKI*#, R. BURDZIK**, G. SIWIEC***, Ł. KONIECZNY**, J. WARCZEK**, P. FOLĘGA**, B. OLEKSIAK***

DISK LASER WELDING OF CAR BODY ZINC COATED STEEL SHEETS

SPAWANIE LASEREM DYSKOWYM BLACH ZE STALI KAROSERYJNEJ OCYNKOWANEJ

Autogenous laser welding of 0.8 mm thick butt joints of car body electro-galvanized steel sheet DC04 was investigated. The Yb:YAG disk laser TruDisk 3302 with the beam spot diameter of 200 μm was used. The effect of laser welding parameters and technological conditions on weld shape, penetration depth, process stability, microstructure and mechanical performance was determined. It was found that the laser beam spot focused on the top surface of a butt joint tends to pass through the gap, especially in the low range of heat input and high welding speed. All test welds were welded at a keyhole mode, and the weld metal was free of porosity. Thus, the keyhole laser welding of zinc coated steel sheets in butt configuration provides excellent conditions to escape for zinc vapours, with no risk of porosity. Microstructure, microhardness and mechanical performance of the butt joints depend on laser welding conditions thus cooling rate and cooling times. The shortest cooling time $t_{8/5}$ was calculated for 0.29 s.

Keywords: car body steel, DC04, laser welding, disk laser, zinc

W artykule opisano wyniki badań procesu spawania laserowego bez materiału dodatkowego złączy doczołowych blach karoseryjnych ocynkowanych DC04 o grubości 0.8 mm. W procesie spawania zastosowano laser stały Yb:YAG TruDisk 3302 z wiązką laserową o średnicy ogniska 200 μm. Badano wpływ parametrów i warunków technologicznych spawania na kształt i głębokość ściegu spoiny, stabilność procesu spawania, mikrostrukturę i właściwości mechaniczne złączy. Stwierdzono, że wiązka laserowa zogniskowana na górnej powierzchni blach wykazuje tendencję do przenikania przez szczelinę złącza, szczególnie przy niskich energiach liniowych i dużych prędkościach spawania. W całym zakresie parametrów złącza były spawane z utworzeniem kanału parowego, a metal spoiny był wolny od porowatości. Wskazuje to, że konfiguracja złącza doczołowego stwarza dogodne warunki do ujścia par cynku, bez ryzyka porowatości spoin. Mikrostruktura, mikrotwardość i właściwości mechaniczne złączy zależą wyraźnie od warunków spawania, a więc szybkości stygnięcia i czasów stygnięcia. Najkrótszy wyznaczony czas stygnięcia $t_{8/5}$ był równy 0.29 s.

1. Introduction

Thin galvanized zinc coated steel sheets are now widely used in the global automotive industry. Sheets of this type are used in the manufacture of automobile bodies in high volume production because of excellent corrosion resistance and relatively low costs [1-10].

The basic, conventional and used for many years method of joining of the car body parts is a resistance spot welding (RSW) [7-12]. In the case of car body parts with larger thicknesses, also the method of gas metal arc welding (GMAW or MIG/MAG) is used. The typical and conventional car body contains approx. 4500 resistance spot welds and also many meters of MIG and MAG weld beads [1,7,11-14]. Both joining methods mentioned above are still used but the extent of their use systematically decreases [1,7]. The reason for this is the continuous introduction of new materials such as advanced automotive steels, galvanized high-strength dual-phase steel, trip steels, increase use of aluminium and composites, "sandwich" steel, and tailored blanks [2-4,7-37]. The conventional resistance and arc welding methods are not proper for welding of new materials and joints of dissimilar materials [38-42]. Therefore, the laser welding is increasingly used in the automotive industry [1,18-22]. The materials and connections techniques in automotive industry have to be considered under many requirements. One of the most important is vibration. That is how there are a lot of research on vibrations [43-48] and it should be analysed during the welding process as well in term of influence on the propagation paths. In addition to laser welding technology, the welding-brazing, hybrid welding, cold joining by forming and clinching, structural adhesive bonding are becoming increasingly important [1,8]. Laser welding offers many benefits such as high welding speed, low heat input, narrow weld and narrow heat affected zone (HAZ), high

* SILESIAN UNIVERSITY OF TECHNOLOGY, FACULTY OF MECHANICAL ENGINEERING, WELDING DEPARTMENT,18A KONARSKIEGO STR., 44-100 GLIWICE, POLAND
** SILESIAN UNIVERSITY OF TECHNOLOGY, FACULTY OF TRANSPORT, 8 KRASIŃSKIEGO STR., 40-019 KATOWICE, POLAND
*** SILESIAN UNIVERSITY OF TECHNOLOGY, FACULTY OF MATERIALS ENGINEERING AND METALLURGY, KRASIŃSKIEGO STR., 40-019 KATOWICE, POLAND
# Corresponding author: aleksander.lisiecki@polsl.pl

precision, reliability, high efficiency, and high productivity, and improved corrosion resistance of welds, compared to the conventional welding methods [5,6]. However, during the laser welding of galvanized steel many defects may occur such as spatter, strong porosities of weld metal, and surface pits, poor fusion and cracks resulted in poor surface quality, and reduced strength, as well as the corrosion resistance [4,7]. The problems during laser welding of galvanized steels are related to the behaviour of zinc coating. The thickness of zinc coating in a case of car body steel sheets is usually approx. 10 μm or occasionally thicker than 20 μm for added protection [6]. In spite of such a small thickness of the coating, zinc tends to evaporate during the welding process because of low boiling point just 906 °C compared to the 1530 °C of steel. In most cases lap joint configuration is used in the automotive industry for laser welding of car body parts, e.g. door panels, roofs to side panels, etc. In lap configuration the pressurized vapours and zinc destabilize the keyhole and the bubbles are easily trapped in the weld metal. The problem of quality assurance is still valid, and the use of this technology in the industry is growing. For example, the Opel factory in Gliwice has implemented the laser welding technology at the end of 2014. Therefore, many researchers in the world are looking for solutions to increase the quality and productivity in this field. A variety of different methods and techniques were elaborated and proposed by researchers. Some of them are very original. For example W. Chen et al. proposed pre-drilling by a pulsed Nd:YAG laser to form vent holes along the weld line and then seam welding in the lap-joint configuration using a continuous wave CO_2 laser [6]. J. Milberg and A. Trautmann produced defect-free overlap joints of galvanized steel using bifocal hybrid laser welding by combining an Nd:YAG laser with a high power diode laser [8,18-25]. S. Iqbal et al. elaborated the novel method of dual beam laser welding [9]. In this method the precursor beam cuts a slot, thus making an exit path for the zinc vapours, while the second beam performs the needed welding. Tzeng Yih-fong investigated the gap-free lap welding of zinc coated steel by pulsed CO_2 laser [5]. He found that the proper selection of welding parameters at pulsed mode of laser beam generation allows producing visually sound welds. L. Mei et al. found that the composition of shielding gas during laser welding of galvanized steel has significant influence on the weld quality [10]. Especially the small addition of oxygen, approx. 2-4%, to argon gas mixture can effectively reduce the tendency of zinc to evaporation. J. Ma et al. proposed two-pass laser welding of galvanized steel [2]. The first pass is based on a defocused laser spot that scans across the top of the overlapped sheets and heats the zinc coating at the faying surface to be melted and vaporized, while the second pass is executed with a focused laser spot in order to perform the welding.

A.K. Dasgupta and J. Mazumder investigated the laser welding of zinc coated steel with addition of copper as an alloying material. In this case before the steel is melted, a zinc-copper compound is formed, which has a higher melting point (1083°C) than the boiling point of zinc, so the formation of zinc vapour is avoided [11]. Similar effect may be achieved when a thin aluminium alloy foil is set along the weld line at the interface of metal sheets in order to alloy the zinc [12, 22].

The most original technique for laser welding of galvanized steel sheets was proposed by S. Yang and Z. Chen et al. [12,13]. They elaborated a suction device with a nozzle to provide highly pressurized zinc vapour to escape.

However, in industrial practice the most commonly used solution is introducing a joint gap between the sheets so as to provide escape route for zinc vapours [1,7,13-18]. However, providing a homogeneous gap requires complex clamping systems and usually a spacer as an additional material, or projections made in one of the sheets to be welded. Therefore, it is difficult to provide high repeatability and quality of welding in high volume production [1,7,19-25].

Another problem during laser welding of zinc coated steel sheets is sever Zn plasma formation over the keyhole. Problems related to the Zn plasma are described by W. Chen, et al. [6]. They found that the Zn plasma plume disrupts the absorption and scatters the laser beam. The high number of publications concerning the laser welding of zinc coated steel indicates that the process is thoroughly tested and well described. Most of these publications relate to the welding of overlap joints by means of gaseous CO_2 and solid state (rod) Nd:YAG lasers [16-29]. However, there are few publications on butt welding of car body zinc coated steel sheets. In addition, thanks to the continuous and dynamic development in physics and optics of lasers, new types of laser devices are available now. The most modern lasers introduced for welding are the fibre and disk lasers [14-18,20]. They are characterized by a number of advantages compared to the conventional CO_2 end rod Nd:YAG lasers [26,29].

Therefore, the studies of butt joints welding of car body double sided zinc coated steel sheets with a thickness of 0.8 mm, by means of the modern disk laser, were undertaken by authors of the manuscript.

The effect of laser welding parameters on the process stability, microstructure of fusion zone and heat affected zone, microhardness distribution, mechanical properties such as tensile strength and bending angle of test joints have been evaluated.

2. Material and experimental procedure

The material used was 0.8 mm thick electro-galvanized steel sheet DC04 with approx. 10 μm pure zinc coating on both sides. The chemical composition of steel substrate and mechanical properties are given in Table 1 and 2, and in Fig. 1. Samples in dimension of 200.0 x 110.0 mm were cut from a flat sheet 0.8 mm thick by a mechanical guillotine. A disk laser Yb:YAG TRUMPF TruDisk 3302 with maximum output power 3300 W and beam parameter product (BPP) 8.0 mm·mrad was applied for this study. The detailed technical data of the applied laser are given in previous manuscripts [14-18]. The circular laser beam having a wavelength of 1.03 μm was delivered into the focusing optics via fiberglass. The focusing optics was configured in such a way to achieve the spot beam diameter equal to 200 μm. The laser welding head was mounted on the vertical drive, while the plates to be welded were mounted on the "x,y" table of experimental CNC controlled stand, Fig. 2. During the welding tests the laser head was stationary, while the plates were moved linearly. Based on the experience of previous laser welding studies, the laser beam was focused on the top surface of butt joints to provide the highest welding speed.

In order to determine the parameters for autogenous laser welding of the 0.8 mm thick steel sheets, first the bead-on-plate welding trials were carried out. At the stage of bead-on-plate welding the influence of laser output power and welding speed, thus the heat input of welding (defined as the ratio of laser power and welding speed) on the penetration depth, shape of the weld and process stability was determined. The parameters and technological conditions of bead-on-plate welding tests are given in Table 3. Then, based on the results of bead-on-plate welding, the parameters for butt joints welding were chosen, ensuring full penetration of the 0.8 mm thick joint at high speed of welding.

Laser welding trials were carried out with the sheets in the butt-joint configuration using a clamping device to eliminate any distortion or displacement during laser welding, Fig. 2.

Argon was used as the shielding gas during the welding process with a constant flow rate of 15.0 l/min. Prior to welding, the edges of sheets, as well as the adjacent areas with a width of 15 mm were cleaned and decreased by acetone. The parameters and technological conditions of test joints welding are given in Table 4.

After welding, first the visual inspection was performed, and next the weld appearance and topography were examined using an optical microscope (OM). In the next step samples were cut perpendicularly to the joint axis at the mid-length of the joint for further metallographic examinations. Samples were mounted in resin (thermosetting), grinded and polished, then etched by Adler reagent for macroscopic observations, and by Nital solution (3.0%) to reveal the microstructure of the welded joints. Mechanical tests and microhardness measurements were also performed. Vicker's microhardness at a load 200 g was measured on cross-section in the middle of sample thickness.

TABLE 1

Chemical composition of the zinc coated steel sheet substrate, Fig. 1

Grade : DC04 steel	**Content % wt.**					
	C	Mn	Si	P	S	other
According to EN10130-2006	max 0.08	max 0.4	-	max 0.03	max 0.03	-
According to the certificate	0.02	0.14	0.008	0.006	0.014	Al. 0.033 Ti 0.087

TABLE 2

Mechanical properties of the zinc coated steel sheet substrate (for cold re-rolled condition), Fig. 1

Grade	Tensile strength Rm, MPa	Yield point $Rp_{0.2}$, MPa	Rm/Rp	Fracture elongation A_{80}, %	Vertical anisotropy r_{min}	Work hardening exponent $n_{10\text{-}20}$	Bending angle α, °
DC04	270÷350	140÷210	0.62	38	1.6	0.18	180

TABLE 3

Parameters of bead-on-plate welding of 0.8 mm thick zinc coated steel sheet DC04 by disk laser TruDisk 3302

Bead No.	Laser power, W	Welding speed, mm/min (mm/s)	Heat input, J/mm	Width of the HAZ, mm	Width of the weld face, mm	Width of the weld root, mm	Shape of FZ	Remarks
B1	750	5000 (83.3)	9.00	0.13	0.47	0.23	Y	NO,FP,FF,NS
B2	750	4000 (66.6)	11.2	0.20	0.57	0.37	Y/V	NO,FP,FF,NS
B3	750	3000 (50)	15.0	0.37	0.73	0.53	V	NO,FP,FF,NS
B4	750	2000 (33.3)	22.5	0.41	0.83	0.66	V	NO,FP,FF,NS
B5	750	1000 (16.6)	45.2	0.51	1.13	1.08	II	NO,FP,FF,NS
B6	750	500 (8.33)	90.0	-	-	-	-	BT
B7	750	750 (12.5)	60.0	0.76	1.41	1.29	II	FP,FF,NS
B8	2000	6000 (100)	20.0	0.16	0.5	0.5	X	NO,FP,FF,NS
B9	1500	6000 (100)	15.0	0.18	0.51	0.52	X	NO,FP,FF,NS
B10	1000	6000 (100)	10.0	0.16	0.5	0.4	X/I	NO,FP,FF,NS
B11	750	6000 (100)	7.50	0.1	0.46	0.25	X	NO,FP,FF,NS
B12	500	6000 (100)	5.00	0.07	0.43	-	V	LP

Remarks, other parameters of bead-on-plate welding: wavelength of laser radiation 1.03 μm, focal length of focusing lens: 200.0 mm, focal length of collimator lens: 200.0 mm, fiber core diameter: 200.0 μm, nominal beam spot diameter: 200.0 μm, shielding nozzle diameter: 8.0 mm, shielding gas: Ar (99.999%), gas feed rate 15 l/min, Quality assessment of the welds: FP – full penetration, BT - burn through, LP – lack of penetration, NO – no oxidation, FF – flat wed face, NS – no spatter

TABLE 4

Parameters of laser welding of 0.8 mm thick butt joints of zinc coated steel DC04 by disk laser TruDisk 3302

Test butt joint	Output laser power, W	Welding speed, mm/min (mm/s)	Heat input, J/mm	Width of the weld face, mm	Width of the weld root, mm	Remarks
J1	1000	4000 (66.6)	15	0.8	0.78	NP,FC,RC
J2	1000	3000 (50)	20	0.73	0.85	FC,RC,JD,UF
J3	1000	2000 (33.3)	30	0.92	0.96	NP,JD

Remarks, other parameters of butt joints laser welding are given in Table 3, Quality assessment of the welds: NP – no porosity, FC – weld face concavity, RC – weld root concavity, JD – joint distortion, UF – uneven weld face

Samples for tensile tests were cut perpendicularly to the joint axis and shaped by milling with intensive water cooling to avoid the effect of heat on the performance of test samples. Static tensile tests were carried out at room temperature.

Finally the technological bend tests of the laser welded joints were performed on samples having a width of 20.0 mm. Samples for the bend test were cut in the same way as the samples for tensile tests, perpendicularly to the joint axis.

Fig. 1. Microstructure of the 0.8 mm thick electro-galvanized steel sheet DC04, 3% Nital etched, Table 1

Fig. 2. A view of the clamping device applied for laser welding of 0.8 mm thick electro-galvanized steel sheet DC04

3. Characteristic of bead-on-plate welds

In the initial stage of the study the influence of laser welding speed and laser output power on the fusion zone (FZ) shape and penetration depth was investigated. Under this approach, the aim was to determine the minimum heat input of laser butt joint welding at the maximum welding speed. Therefore, the laser beam was focused on the top surface of the 0.8 mm thick sheets to provide maximum power density, and thus maximum penetration depth at a given laser output power. Results of the bead-on-plate laser welding tests showed that the heat input required for full penetration of the butt joint of 0.8 mm thick zinc coated steel sheets DC04 is relatively low and equals approx. 7.5 J/mm, at the laser power just 750 W, and so high welding speed 6.0 m/min (100 mm/s), as shown in Fig. 4a and Table 3.

Previous experience in laser welding of thin steel sheets indicates that the mechanism of butt joint welding is slightly different, compared to the bead-on-plate welding, and also the stability of butt joint welding may be significantly lower. Therefor the welding speed of 6.0 m/min was set as the maximum welding speed, despite a significant laser power reserve (up to 3.3 kW) and possibility of further increasing the welding speed.

Fig. 3. A view of the bead-on-plate welds produced on the 0.8 mm thick electro-galvanized steel sheet DC04 by a disk laser, Table 3

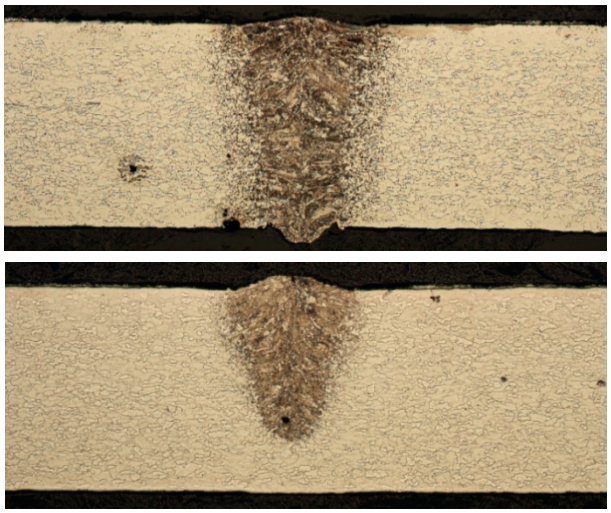

Fig. 4. Cross sections of the bead-on-plate welds produced on the 0.8 mm thick electro-galvanized steel sheet DC04 by a disk laser, Table 3; a) bead B11 (750 W, 6.0 m/min, 7.5 J/mm), b) bead B12 (lack of penetration)

It was also found that the range of heat input required for full penetration of the 0.8 mm thick sheet is very wide from approx. 7.5 to 60 J/mm, in the investigated range of laser power and welding speed, Table 3. Further increase of

the heat input to 90 J/mm resulted in severe burn through, as shown in Fig. 3 (bead B6, Table 3). The visual inspection of bead-on-plate welds revealed that the single beads produced on the 0.8 mm thick zinc coated steel sheet DC04, at the heat input up to approx. 20 J/mm (B1-B4, B8-B11, Table 3), are very narrow, and simultaneously the damage of zinc coating is negligible.

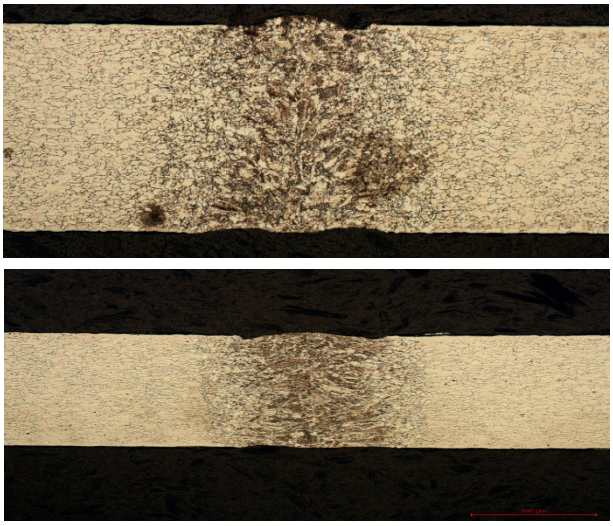

Fig. 5. Cross sections of the bead-on-plate welds produced on the 0.8 mm thick electro-galvanized steel sheet DC04 by a disk laser at the same heat input of 15 J/mm, Table 3; a) bead B3 (750 W, 3.0 m/min), b) bead B9 (1500 W, 6.0 m/min)

In the case of bead-on-plate welds produced at the heat input up to 20 J/mm the weld width doesn't exceed 0.5-0.7 mm, Fig. 3-6, Table 3. Surfaces of the weld faces as well as weld roots are flat and even, without any spatter traces of zinc neither steel vapours or slag, Fig. 3. It is worth mentioning that during the bead-on-plate laser welding tests a blue/white plasma plume was observed over the laser beam interaction area. The plasma plume is characteristic for laser welding at the keyhole mode (deep penetration). The minimum level of laser output power applied during bead-on-plate welding tests was set at 500 W. Taking into account that the diameter of the laser beam spot is equal to 200 μm, the power density at the lowest output power of 500 W is $3.9 \cdot 10^5$ W·cm^{-2}. So even at the minimum laser power the power density was over the threshold required for a keyhole welding of structural mild or low alloyed steel sheets [14]. Figures from 4 to 6 show the macrostructure of the bead-on-plate welds. The shape and the depth/width ratio of the individual beads confirm that most of the bead-on-plate welds were produced at the keyhole welding mode, Fig. 4-6.

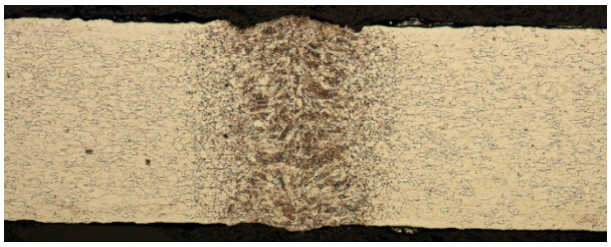

Fig. 6. Cross sections of the bead-on-plate welds produced on the 0.8 mm thick electro-galvanized steel sheet DC04 by a disk laser at very similar heat input, Table 3; a) bead B4 (750 W, 2.0 m/min, 22.5 J/mm), b) bead B8 (2000 W, 6.0 m/min, 20 J/mm)

Close observation of the macrographs of bead-on-plate welds showed that the three characteristic regions, such as fusion zone (FZ), heat affected zone (HAZ), and the base metal (BM), are easy to identify, as can be seen in Fig. 4 to 6. The fusion lines (FL) are very clear and additionally the width of the individual regions of welds are easy to estimate and measure, as given in Table 3. As can be seen, the shape and the depth/width ratio of the individual beads depend on the laser welding parameters, thus thermal conditions of heating, melting and subsequent solidification. Laser bead-on-plate welding of the 0.8 mm thick DC04 steel sheet at high speed 5.0 m/min, and simultaneously low power 750 W (heat input just 9 J/mm), resulted in "Y" weld configuration, Table 3. The depth/width ratio in this case is 1.7, so typical for a keyhole laser welding. Reduction of welding speed, at unchanged laser power, resulted in changing the shape of the weld. For example the bead-on-plate weld produced at 2.0 m/min (B4, 22.5 J/mm, Table 3) has a "V" shape of the fusion zone and the depth/width ratio in this case is just 0.96, but still typical for a keyhole laser welding mode. Whereas, the bead-on-plate weld produced at 1.0 m/min (B5, 45.2 J/mm, Table 3) has a columnar "I" shape at the depth/width ratio 0.7, which is close to the limit for the keyhole.

There were no signs of porosity or any instability of the bead-on-plate laser welding process. It must therefore be concluded that the laser welding of zinc coated steel sheets in butt configuration provides excellent conditions to escape for zinc vapours. The process of laser bead-on-plate welding was very stable in the range of investigated parameters, so no evidence was found to disrupting the laser beam by the plasma plume.

4. Structure and properties of butt joints

After the detailed analysis of the effect of laser bead-on-plate welding on the penetration depth and shape of fusion zone, next the trials of butt joints welding were undertaken. The first attempts to weld of butt joints of the 0.8 mm thick zinc coated DC04 steel sheets have revealed significant differences and difficulties in the process.

The first trials of laser welding at the laser power of 750 W and welding speed of 5.0 m/min were unsuccessful because of insufficient heating and just slight melting of the sheets edges. The reason for this was small laser beam diameter of 200 μm, which just "flew" through the joint gap.

Despite the precision cutting of the samples for welding and accurate fit prior to welding by the stiff clamping device,

in some areas the gap width was up to 0.1 mm, so exactly 50% of the laser beam spot diameter. Thus, due to the high precision of the laser beam spot, as a welding heat source, the required accuracy for joints preparation must be adequate to the beam diameter. It was not possible to ensure greater accuracy of sheet edges preparation and less width of the gap than 0.1 mm. Thus, in order to allow welding, it was necessary to correct the range of processing parameters.

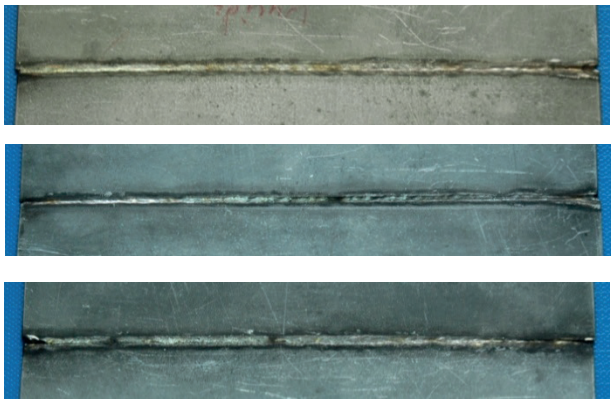

Fig. 7. A view of the weld face (top surface) of the test joints of 0.8 mm thick electro-galvanized steel sheet

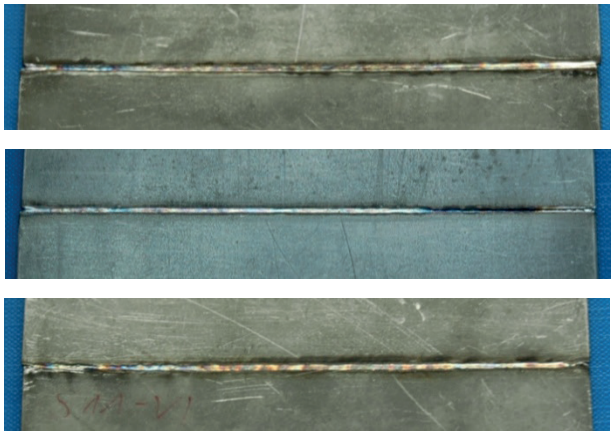

Fig. 8. A view of the weld root (bottom) of the test joints of 0.8 mm thick electro-galvanized steel sheet DC04, autogenously welded by a disk laser (Table 4); a) J1, b) J2, c) J3

Full and proper penetration of the entire length of the butt joint requires higher heat input of welding, at least 15 J/mm, at the laser output power 1.0 kW and welding speed 4.0 m/min, as shown in Table 4. For comparison the minimum heat input required for full and proper penetration of the sheet during bead-on-plate welding was just approx. 7.5 J/mm, so twice lower, Table 3. The increased heat input during butt joints welding resulted in increasing of the volume of melt pool. The molten metal flows into the gap between the sheets and fulfils it. Therefore the conditions for absorption of laser energy and proper fusion of both sheets are favourable.

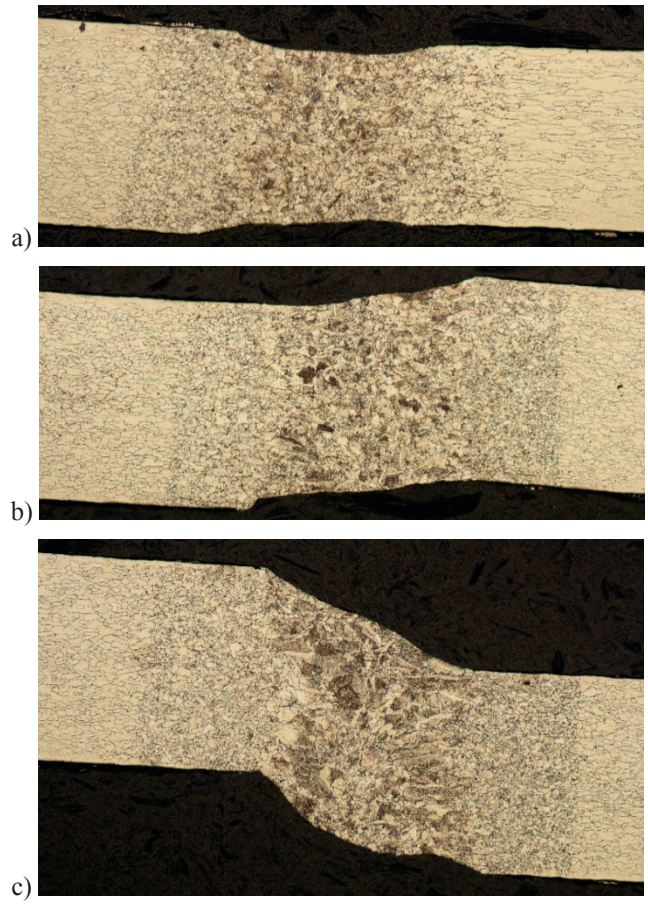

Fig. 9. Macrographs of butt joints of 0.8 mm thick electro-galvanized steel sheet DC04, autogenously welded by a disk laser (Table 4); a) J1, b) J2, c) J3

The weld face of the butt joint J1 produced at the minimum heat input of 15 J/mm, laser power 1.0 kW, and welding speed 4.0 m/min is flat and even, as can be seen in Fig. 7a. Similarly the root of this joint is flat and shiny, Fig. 8a. In turn, the faces of joints J2 and J3 produced at higher heat input are uneven, Fig. 7a,b. The surface of weld face J2 is concave and there are some undercuts, as can be seen in Fig. 7b.

Additionally, subsequent studies showed that, despite a rigid mounting of the steel sheets, it is difficult to provide laser welding of the butt joints without distortion, Fig. 9. As can be seen in Fig. 9 the extent of butt joints deformation is directly proportional to the thermal conditions of laser welding, thus heat input of welding. The butt joint J1 produced at the lowest heat input of 15 J/mm has not been deformed, Fig. 9a, Table 4.

While the joint J2 laser welded at the heat input higher by approx. 30%, compared to the joint J1, has been slightly deformed, Fig. 9b, Table 4. Most intense deformation can be observed in a case of the joint J3 welded at the highest heat input of 30 J/mm, so twice higher compared to the joint J1, Fig. 9c, Table 4.

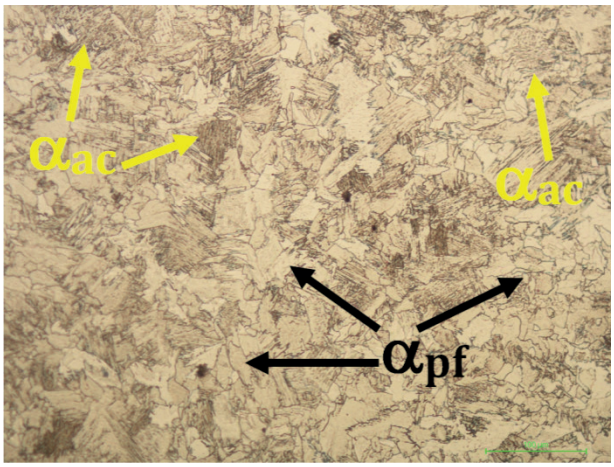

a)

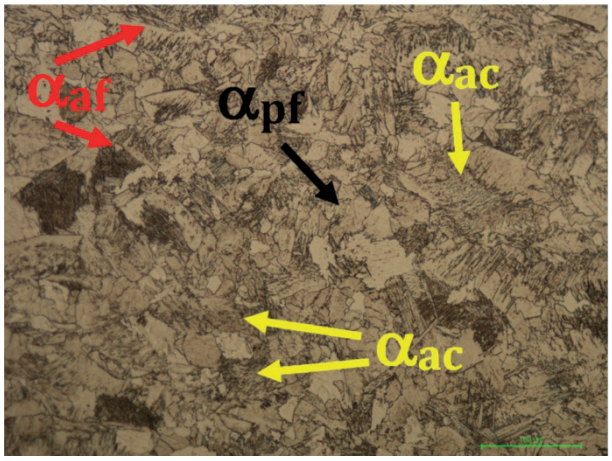

b)

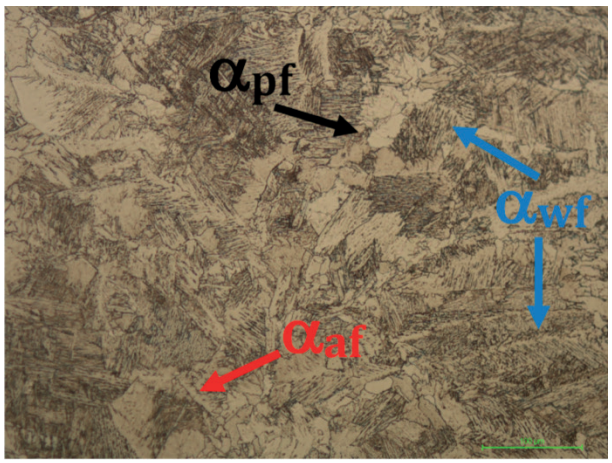

c)

Fig. 10. Microstructure of the weld metal of 0.8 mm thick butt joints of electro-galvanized steel sheet DC04, autogenously welded by a disk laser (Table 4); a) J1, b) J2, c) J3, αpf – polygonal ferrite, αwf – Widmanstatten ferrite, αaf – allotriomorphic ferrite, αac – acicular ferrite

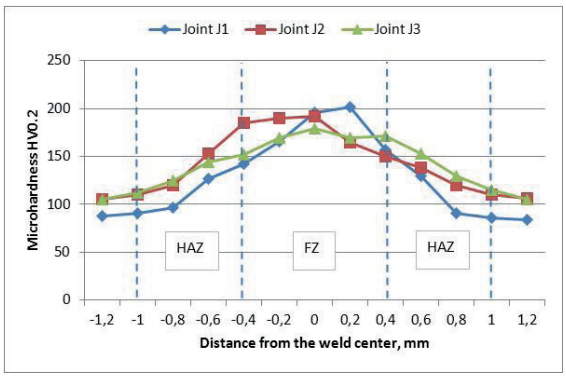

Fig. 11. Microhardness distribution (profile) across the butt joints of 0.8 mm thick electro-galvanized steel sheet DC04, welded by a disk laser (Table 4)

Width of the HAZ is in a range of 0.2-0.4 mm for the test butt joints. The microstructure in the HAZ is very fine grained. This is a result of metal recrystallization at very rapid cooling rates. The cooling times $t_{8/5}$ in HAZ were calculated in such a way described in details in the Ref 14. The calculations showed that the cooling time $t_{8/5}$ in a case of the joint J1 welded at the minimum heat input is extremely short approx. 0.3 s, as given in Table 5. On the other hand the cooling time $t_{8/5}$ calculated for the joint J3 welded at the highest heat input doesn't exceed 1.2 s, Table 5. Microstructure of the DC04 steel consists of ferrite with clear segregation shearing lines, which are the result of a plastic deformation during steel coil rolling, Fig. 1,4-6,9,10. Figure 10 shows the microstructure in the fusion zone of the individual butt joints, Table 4. As can be seen, the microstructure of weld metal is also correlated to the conditions of laser welding, thus heat input. Microscopic observations confirmed that the weld metal is free of any imperfections such as porosity, inclusions, or cracks, as widely reported in a case of overlap laser welding of zinc coated car body steel. The weld metal consists of different types and size of ferrite, as shown in Fig. 10. At low heat input of laser welding the cooling rate of weld metal is rapid. Under such conditions the share of acicular ferrite is higher, as can be seen in Fig. 10a. The weld metal of the joint J1, produced at the minimum heat input of 15 J/mm, consists mainly of polygonal ferrite but also significant share of acicular ferrite may be observed, Fig. 10a. The microstructure of the joint J2, produced at higher heat input, is slightly different, Fig. 10b. In this case, beside the polygonal and acicular ferrite, additionally the allotriomorphic ferrite was identified, Fig. 10b. The microstructure is associated with a lower cooling rate, Table 5. Quite different is the microstructure of the weld metal in a case of the joint J3, produced at the highest heat input of

TABLE 5
Values of the calculated cooling times $t_{8/5}$ during autogenous laser welding of butt joints of 0.8 mm thick electro-galvanized steel sheet DC04, welded by a disk laser (Table 4)

Test butt joint	Output laser power, W	Welding speed, mm/min (mm/s)	Heat input, J/mm	HAZ width, mm	Cooling time $t_{8/5}$, s
J1	1000	4000 (66.6)	15	0.37-0.39	0.29
J2	1000	3000 (50.0)	20	0.4-0.42	0.52
J3	1000	2000 (33.3)	30	0.45-0.5	1.16

30 J/mm, Fig. 10c. In this case the share of acicular ferrite is significantly lower, Fig. 10c. In addition the size of polygonal ferrite grains is higher, and also the share of Widmanstatten ferrite increased significantly, Fig. 10c.

After measuring the microhardness distribution (profile) across the butt joints found that it is also clearly dependent on the welding conditions, thus microstructure of the weld metal and heat affected zone, Fig. 11. As can be seen in the microhardness graph, the Vickers microhardness measured in the region of base metal is approx. 90-100 HV0.2, Fig.11. In every case the maximum values of microhardness were measured in the region of weld metal (fusion zone FZ). Then, the microhardness decreases gradually from the fusion line (FL) to base metal (BM), in the region of HAZ, Fig. 11.

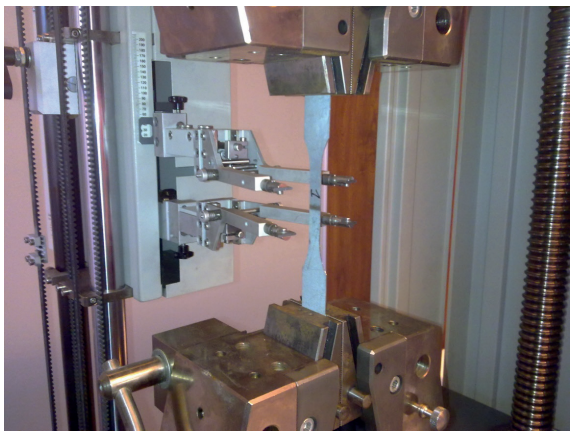

Fig. 12. A view of the tensile sample during static tensile test of a butt joint of 0.8 mm thick electro-galvanized steel sheet DC04

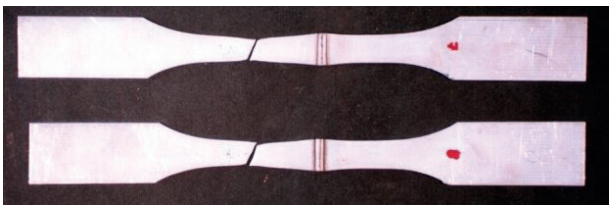

Fig. 13. A view of the broken samples from the tensile tests of the butt joint J1 welded at 1.0 kW and welding speed of 4.0 m/min (heat input of 15 J/mm, Table 4)

Maximum value of microhardness approx. 205 HV0.2 was determined in the centre of FZ (weld metal) of the joint J1, welded at the highest welding speed of 4.0 m/min, and the lowest heat input just 15 J/mm, Fig. 11. Lower value of microhardness approx. 185-190 HV0.2 was determined in the case of butt joint J2, welded at higher heat input of 20 J/mm, Fig. 11. On the other hand, in the case of the third butt joint J3, welded at the highest heat input of 30 J/mm, the microhardness measured in weld metal was significantly lower approx. 175-180 HV 0.2, especially compared to the joint J1, as can be seen in Fig. 11. After the microhardness measurements mechanical tests were performed by means of a static tensile test and a technological bend test, Fig. 12,13 and Table 6,7. As can be seen, all of the tested samples were broken in the base metal, away from the fusion zone and heat affected zone, Fig. 13, Table 6. Thus, the joints strength is not less than the strength of the base metal of 0.8 mm thick DC04 steel sheet, as can be seen in Table 2.

TABLE 6

Results of the tensile strength test of butt joints of 0.8 mm thick electro-galvanized steel sheet DC04, welded by a disk laser, Fig. 13, Table 4

Joint No.	Sample No.	Tensile strength Rm, MPa	Place of break
J1	J1A	301	Base metal
	J1B	287	
J2	J2A	294	
	J2B	291	
J3	J3A	281	
	J3B	298	

TABLE 7

Results of the technological bend test of butt joints of 0.8 mm thick electro-galvanized steel sheet DC04, welded by a disk laser, Table 4

Joint No.	Test type	Bending angle, °	Remarks
J1	root bend	180	no cracks
	face bend		
J2	root bend		
	face bend		
J3	root bend		
	face bend		

Similarly in the case of the technological bend test, two samples were prepared for each of the examined butt joints (one for root and one for weld face bending). The bending angle reached the maximum value of 180° for every tested sample, Table 7. Therefore, results of the technological bend test confirmed high mechanical performance of the butt joints of 0.8 mm thick electro-galvanized steel sheet DC04, welded by a disk laser.

5. Conclusions

In this study, autogenous laser welding of butt joints of 0.8 mm thick zinc coated steel DC04 with a disk laser was investigated. Based on the results a few conclusions can be drawn. Accuracy of sheet edges preparation and positioning of the laser beam along the joint line are crucial parameters in a case of laser welding of butt joints of thin steel sheets. Despite the precise preparation of the edges of sheets to be welded, the width of the joint gap was up to 0.1 mm. In this case, the laser beam spot with a diameter of 200 μm, focused on the top surface of a joint, tends to pass through the gap, especially in the low range of heat input and high welding speed. Therefore butt laser welding requires higher heat inputs, compared to bead-on-plate welding. Improvement in this situation would provide a defocusing of the laser beam, but at the expense of efficiency and effectiveness of the process. Additionally, despite a rigid mounting of the steel sheets, it is difficult to eliminate the distortions of butt joints of thin sheets. All test welds were free of porosity. This means that the keyhole laser welding

of zinc coated steel sheets in butt configuration provides excellent conditions to escape for zinc vapours. Microstructure, microhardness and mechanical performance of the butt joints depend on laser welding conditions, thus cooling rate and cooling times $t_{8/5}$. All the test butt joints exhibit excellent tensile strength of the base metal level.

REFERENCES

[1] A. Ribolla, et al. The use of Nd:YAG laser weld for large scale volume assembly of automotive body in white, Journal of Materials Processing Technology **164–165**, 1120–1127 (2005).

[2] J. Ma,etal., Two-pass laser welding of galvanized high-strength dual-phase steel for a zero-gap lap joint configuration, Journal of Materials Processing Technology **213**, 495– 507 (2013).

[3] U.Reisgen, et al., Shielding gas influences on laser weldability of tailored blanks of advanced automotive steels, Applied Surface Science **257**, 1401–1406 (2010).

[4] Yi Zhang, et al., Characteristics of zinc behavior during laser welding of zinc ''sandwich'' sample, Optics & Laser Technology **44**, 2340–2346 (2012).

[5] Tzeng Yih-fong, Gap-free lap welding of zinc-coated steel using pulsed CO_2 laser, Int. J. Adv. Manuf. Technol. **29**, 287–295 (2006).

[6] W. Chen, et al., CO_2 laser welding of galvanized steel sheets using vent holes, Mat. and Des. 30, 245-251 (2009).

[7] M. Lifang, et al., Comparative study on CO_2 laser overlap welding and resistance spot welding for galvanized steel, Mat. and Des. **40**, 433-442 (2012).

[8] J. Milberg, A. Trautmann, Defect-free joining of zinc-coated steels by bifocal hybrid laser welding, Prod. Eng. Res. Devel. **3**, 9–15 (2009).

[9] S. Iqbal, et al., Dual beam method for laser welding of galvanized steel: Experimentation and prospects, Optics & Laser Technology **42**, 93–98 (2010).

[10] L. Mei, et al., Research on laser welding of high-strength galvanized automobile steel sheets, Optics and Lasers in Engineering **47**, 1117–1124 (2009).

[11] A.K. Dasgupta, J. Mazumder, Laser welding of zinc coated steel: an alternative to resistance spot welding. Science and Technology of Welding and Joining **13**, 289–293 (2008).

[12] S. Yang, et al., Vacuum-Assisted Laser Welding of Zinc-Coated Steels in a Gap-Free Lap Joint Configuration, Welding Journal **92**, 197-204 (2013).

[13] Z. Chen, et al., A study of fiber laser welding of galvanized steel using a suction method, Journal of Materials Processing Technology **214**, 1456–1465 (2014).

[14] A. Lisiecki, Welding of thermomechanically rolled fine-grain steel by different types of lasers, Arch. Metall. Mater. **59**(4), 1625-1631 (2014).

[15] A. Lisiecki, Diode laser welding of high yield steel, Proceedings of SPIE, Laser Technology 2012: Application of Lasers, **8703** (2013).

[16] A. Lisiecki: Welding of titanium alloy by Disk laser. Proceedings of SPIE, Laser Technology, Applications of Lasers, **87030** (2013).

[17] A. Lisiecki, Titanium Matrix Composite Ti/TiN Produced by Diode Laser Gas Nitriding, Metals **5**(1), 54-69 (2015), doi:10.3390/met5010054.

[18] D. Janicki, Disk laser welding of armor steel, Arch. Metall. Mater. **59**(4), 1641-1646 (2014).

[19] A. Kurc-Lisiecka, W. Ozgowicz, W. Ratuszek, J. Kowalska: 'Analysis of Deformation Texture in AISI 304 Steel Sheets', Sol. St. Phenomena **203-204**, 105-110 (2013).

[20] M. Bonek, The investigation of microstructures and properties of high speed steel hs6-5-2-5 after laser alloying, Arch. Metall. Mater. **59**(4), 1647-1651 (2014).

[21] R. Burdzik, Ł. Konieczny, Z. Stanik, P. Folega, A. Smalcerz, A. Lisiecki, Analysis of impact of chosen parameters on the wear of camshaft, Arch. Metall. Mater. **59**(3), 957-963 (2014).

[22] J. Jezierski, K. Janerka, Parameters of a Gas-Solids Jet in Pneumatic Powder Injection into Liquid Alloys with a Non-Submerged Lance, Metalurgija **54**(2), 365-367 (2015).

[23] M. Bonek, L.A. Dobrzański,Characterization performance of laser melted commercial tool steels, Mat. Sci. Forum **654-656**, 1848-1851 (2010).

[24] W. Sitek, L.A. Dobrzański, Comparison of hardenability calculation methods of the heat-treatable constructional steels, J. Mat. Proc. Tech. **64**(1-3), 117-126 (1995).

[25] J. Górka, Analysis of simulated welding thermal cycles S700MC using a thermal imaging camera, Adv. Mat. Res. ISI Proceedings **837**, 375-380 (2014).

[26] J. Bodzenta, A. Kaźmierczak, T. Kruczek, Analysis of thermograms based on FFT algorithm, Journal de Physique **IV 129**, 201-206 (2005).

[27] A. Grajcar, M. Różański, S. Stano, A. Kowalski, B. Grzegorczyk: 'Effect of Heat Input on Microstructure and Hardness Distribution of Laser Welded Si-Al TRIP-Type Steel' Adv. in Mat. Sci. and Eng. 2014 (2014),

[28] M. Musztyfaga, L.A. Dobrzański, S. Rusz, M. Staszuk, Application examples for the different measurement modes of electrical properties of the solar cells, Arch. Metall. Mater. **59**(1) 247-252 (2014).

[29] G. Moskal, A. Grabowski, A. Lisiecki, Laser remelting of silicide coatings on Mo and TZM alloy, Sol. St. Phenomena **226**, 121-126 (2015). doi:10.4028/www.scientific.net/SSP.226.121

[30] B. Oleksiak, G. Siwiec, A. Blacha-Grzechnik, J. Wieczorek, The obtained of concentrates containing precious metals for pyrometallurgical processing, Metalurgija **53**(4), 605-608 (2014).

[31] L. Blacha, R. Burdzik, A. Smalcerz, T. Matuła, Effects of pressure on the kinetics of manganese evaporation from the OT4 alloy, Archives Of Metallurgy And Materials **58** (1), 197-201 (2013).

[32] B. Oleksiak, J. Labaj, J. Wieczorek, A.Blacha–Grzechnik, R. Burdzik, Surface tension of cu-bi alloys and wettability in a liquid alloy - refractory material - gaseous phase system, Arch. Metall. Mater. **59**(1), 281-285 (2014).

[33] G. Golański, A. Zieliński, J. Słania, J. Jasak, Mechanical Properties of VM12 steel after 30 000hrs of ageing at 600°C temperature, Arch. Metall. Mater. **59**(4), 1357-1360 (2014).

[34] G. Golański, P. Gawień, J. Słania, Examination of Coil Pipe Butt Joint Made of 7CrMoVTib10 - 10(T24) Steel After Service, Arch. Metall. Mater. **57**(2), 1067–1070 (2012).

[35] G. Golanski, J. Slania, Effect of different heat treatments on microstructure and mechanical properties of the martensitic GX12CrMoVNbN9-1 cast steel, Archives of Materials and Metallurgy **58**(1), 25-30 (2013).

[36] A.N. Wieczorek, The role of operational factors in shaping of wear properties of alloyed Austempered Ductile Iron. Part I. Experimental studies abrasive wear of Austempered Ductile Iron (ADI) in the presence of loose quartz abrasive. Archives of Metallurgy and Materials **59**(4), 1665-1674 (2014).

[37] A.N. Wieczorek, The role of operational factors in shaping of wear properties of alloyed Austempered Ductile Iron. Part II. An assessment of the cumulative effect of abrasives processes and the dynamic activity on the wear property of Ausferritic Ductile Iron. Archives of Metallurgy and Materials **59** (4), 1675-1683 (2014).

[38] J. Górka, Weldability of thermomechanically treated steels having a high yield point, Arch. Metall. Mater. **60**(1) 471-477 (2015).

[39] T. Węgrzyn, J. Piwnik, B. Łazarz, D. Hadryś, Main micro-jet cooling gases for steel welding, Arch. Metall. Mater. **58**(2), 555–557 (2013).

[40] T. Węgrzyn, J. Mirosławski, A. Silva, D. Pinto, M. Miros, Oxide inclusions in steel welds of car body, Mat. Sci. Forum **6**, 585-591 (2010).

[41] T. Węgrzyn, J. Piwnik, D. Hadryś. Oxygen in steel WMD after welding with micro-jet cooling, Arch. Metall. Mater. 58(4), 1067–1070 (2013).

[42] G. Golański, J. Jasak, J. Słania, Microstructure, properties and welding of T24 steel - critical review, Kovove Materialy **52**, 99-106 (2014).

[43] R. Burdzik,Ł. Konieczny, Research on structure, propagation and exposure to general vibration in passenger car for different damping parameters, Journal of Vibroengineering **15**(4), 1680-1688 (2013).

[44] R. Burdzik, Research on the influence of engine rotational speed to the vibration penetration into the driver via feet - multidimensional analysis, Journal of Vibroengineering **15**(4), 2114-2123 (2013).

[45] R. Burdzik, Identification of structure and directional distribution of vibration transferred to car-body from road roughness, submitted to Journal of Vibroengineering **16**(1), 324-333(2014).

[46] Z. Dąbrowski, M. Zawisza, The choice of vibroacoustic signal measures, in mechanical fault diagnosis of diesel engines, Solid State Phenomena **236**, 220-227 (2015).

[47] M. Zawisza, Energy loss and the choice of damper of torsional vibration combustion engines, Solid State Phenomena **236**, 188-195 (2015).

[48] J. Pankiewicz, P. Deuszkiewicz, J. Dziurdź, M. Zawisza. Modeling of powertrain system dynamic behavior with torsional vibration damper, Advanced Materials Research **1036**, 586-591 (2014).

Received: 20 October 2014.